Supplementary Information

Experimental section

Materials: trisodium citrate dihydrate ($C_6H_5Na_3O_7 \cdot 2H_2O$), ethyl alcohol ($C_2H_5OH$), Sodium hydroxide (NaOH), nickel sulfate ($NiSO_4 \cdot 6H_2O$), Sodium nitrite ($NaNO_2$), hydrochloric acid (HCl), deionized water (H_2O), salicylic acid ($C_7H_6O_3$), ammonium chloride (NH_4Cl), hydrofluoric acid (HF), potassium hydroxide (KOH), acetone (CH_3COCH_3), sodium hypochlorite solution (NaClO), nitric acid (HNO_3), cobaltous chloride ($CoCl_2 \cdot 6H_2O$), sodium sulfate anhydrous (Na_2SO_4), sodium nitroferricyanide dihydrate ($C_5FeN_6Na_2O \cdot 2H_2O$). All the chemicals utilized were supplied by Chengdu Kelong Ltd in this work. A Zn plate (0.2 mm thick) and a Ti plate (0.5 mm thick) were purchased from Suzhou.

Preparation of TiO$_2$: Firstly, the Ti plate (2.0×4.0 cm^2) was polished with sandpaper until its surface was smooth. Secondly, it was washed sequentially with acetone, alcohol, and deionized water for 10 min. Thirdly, the Ti plate was cleaned with a chemical solution ($HF/HNO_3/H_2O$ = 1: 1: 1) and then washed with deionized water. Fourthly, the clean Ti plate was put into an autoclave containing 5 M NaOH and kept at 180°C for 24 hours. After the autoclave was naturally cooled to room temperature, the impurities on the surface were alternately washed with deionized water and ethanol. After drying, the prepared $Na_2Ti_2O_5$ nanoarrays were immersed in 1 M HCl for ion exchange, and the ion exchange process was kept for 2 h. Then, the obtained $H_2Ti_2O_5$ nanoarrays were washed with deionized water and ethanol. Finally, to get TiO_2 nanograss arrays, $H_2Ti_2O_5$ nanoarrays were annealed in a tube furnace at 450°C for 2 h

under the atmosphere of Ar/H_2.

Preparation of NiCo-TiO$_2$: NiCo alloy was loaded on the surface of TiO_2 by electrodeposition. 0.13 M $NiSO_4 \cdot 6H_2O$, 0.13 M Na_2SO_4, 0.1 M $C_6H_5Na_3O_7 \cdot 2H_2O$, and 0.09 M $CoCl_2 \cdot 6H_2O$ were dissolved in 50 mL deionized water as the electrolyte for electrodeposition. Using a carbon rod as the counter electrode, a calomel electrode as the reference electrode, and a TiO_2 plate as the working electrode, polarize at 60 mA cm^{-2} for 5 min in the above solution. Finally, the Ti plate was taken out and rinsed with water to obtain NiCo-TiO$_2$.

Characterizations: XRD data were acquired by an X-ray diffractometer with Cu Kα radiation (DX-2700B). SEM measurements were carried out on an X-ray diffractometer with Cu Kα radiation (DX-2700B). The absorbance data were measured on UV–vis spectrophotometer of SHIMADZU UV-2600. TEM image was obtained from an atomic-resolution scanning transmission electron microscopy (FEI Talos F200S Super) operated at 200 kV. XPS measurements were performed with Thermo Fischer ESCALAB Xi$^+$.

Electrochemical measurements: All electrochemical measurements were performed on the CHI 660E electrochemical workstation (Shanghai, Chenhua) using a standard Nafion 117 membrane separated H-type three-electrode electrolytic bath. The electrolyte solution consisted of 0.1 M NaOH and 0.1 M $NaNO_2$ using NiCo-TiO$_2$ as the working electrode, graphite rod as the counter electrode, and saturated mercury oxide electrode as the reference electrode. All potentials reported in the work were calibrated for conversion to a reversible hydrogen electrode (RHE). The scanning rate

of LSV is 5mV s^{-1}, and the potential window is −0.2V to −0.7V. The catalyst material of the working electrode was immersed in the electrolyte with an area of 0.25 cm^2.

Determination of NH$_3$: The NH$_3$ concentration in the solution was determined by colorimetry (the obtained electrolyte was diluted 50 times) using the indophenol blue method. In detail, 2 mL of the solution after the reaction was mixed with 2 mL of 1 M NaOH coloring solution containing 5% $C_7H_5NaO_3$ and 5% $C_6H_5Na_3O_7 \cdot 2H_2O$. Then, 1 mL oxidizing solution of 0.05 M NaClO and 0.2 mL catalyst solution of $C_5FeN_6Na_2O$ (1 wt%) were added to the above solution. After standing in the dark for 2 h, the UV–vis absorption spectra were measured. The concentration of NH$_3$ was identified using the absorbance at a wavelength of 655 nm. The concentration-absorbance curve was calibrated using the standard NH$_4$Cl solution with NH$_3$ concentrations of 0, 0.2, 0.5, 1.0, 2.0, 3.0, and 5.0 ppm in 0.1 M NaOH solution. The fitting curve in Fig. S5 (y =0.32909 x+0.04845, R^2=0.9996) shows a good linear relation of absorbance value with NH$_3$ concentration.

Determination of FE and NH$_3$ yield: The FE for NO_2^- reduction was defined as the amount of electric charge used for synthesizing NH$_3$ divided by the total charge passed through the electrode during electrolysis.

FE toward NH$_3$ via NO_2^-RR is calculated by the following equation:

$$FE = (6 \times F \times C_{NH_3} \times V) / (M_{NH_3} \times Q) \times 100\%$$

The total amount of NH$_3$ produced was measured using colorimetric methods. The yield rate of NH$_3$ is calculated as follows:

$$NH_3 \text{ yield rate} = (C_{NH_3} \times V) / (M_{NH_3} \times t \times A)$$

Where F is the Faradaic constant (96485 C mol^{-1}), C_{NH_3} is the concentration of NH$_3$, V is the volume of electrolyte in the anode compartment (45 mL), M_{NH_3} is the molar mass of NH$_3$, Q is the total charge passing the electrode, t is the electrolysis time, and A is the geometric surface area (0.25 cm^2).

Zn-NO$_2^-$ battery preparation: Zn-NO$_2^-$ battery was assembled with NiCo-TiO$_2$ (0.25 cm^2) as the cathode and a polished Zn plate (0.25 cm^2) as the anode. A typical H-type cell that contains 45 mL cathode electrolyte (0.1 M NaOH + 0.1 M NaNO$_2$) and 45 mL anode electrolyte (6 M KOH) separated by Nafion 117 membrane. Zn-NO$_2^-$ battery was tested at room temperature with a CHI 660E electrochemical workstation.
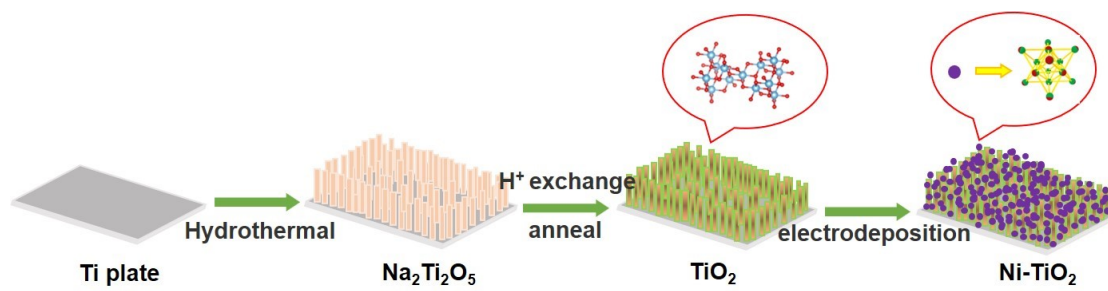
Fig. S1 Schematic diagram of the synthesis of NiCo-TiO$_2$.
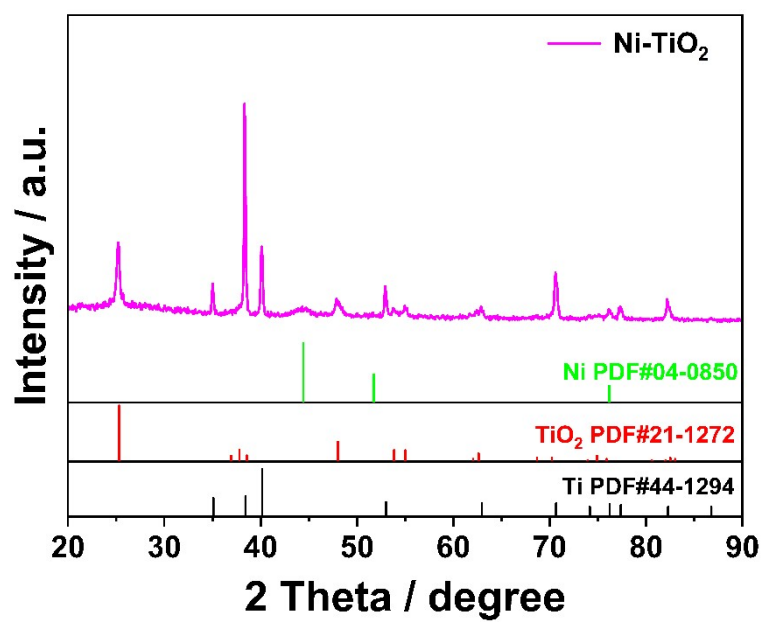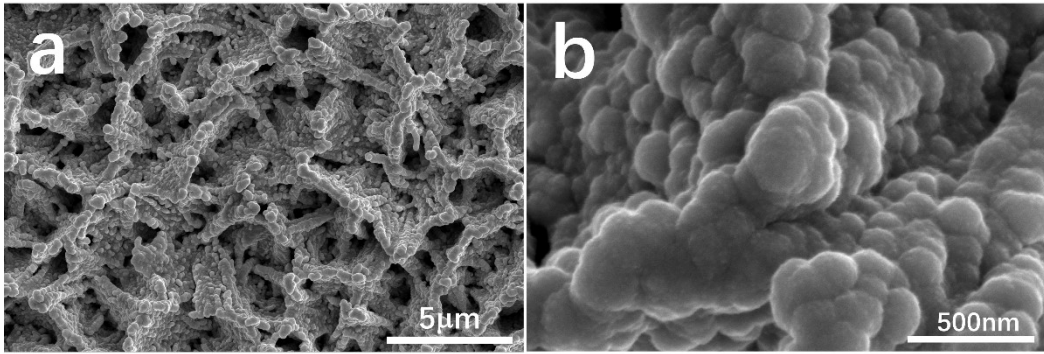
Fig. S2 XRD spectrum of Ni-TiO$_2$.

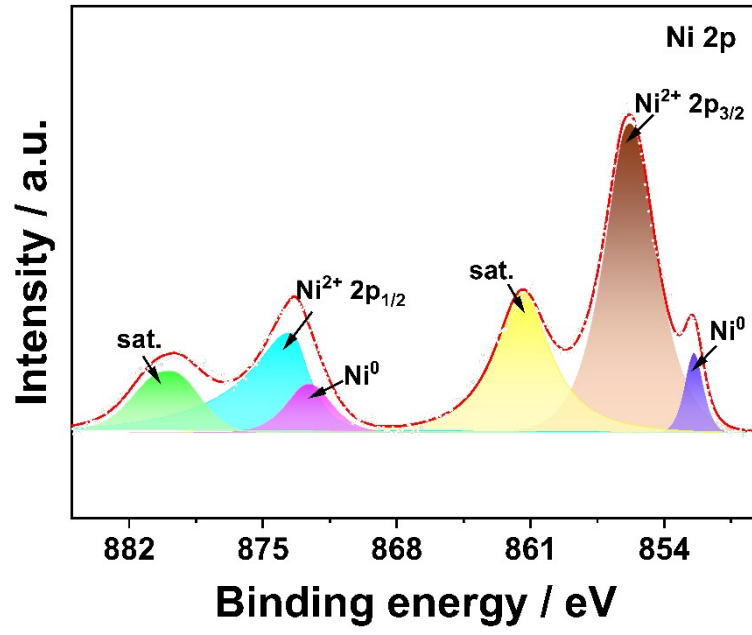Fig. S3 SEM images of Ni-TiO$_2$.
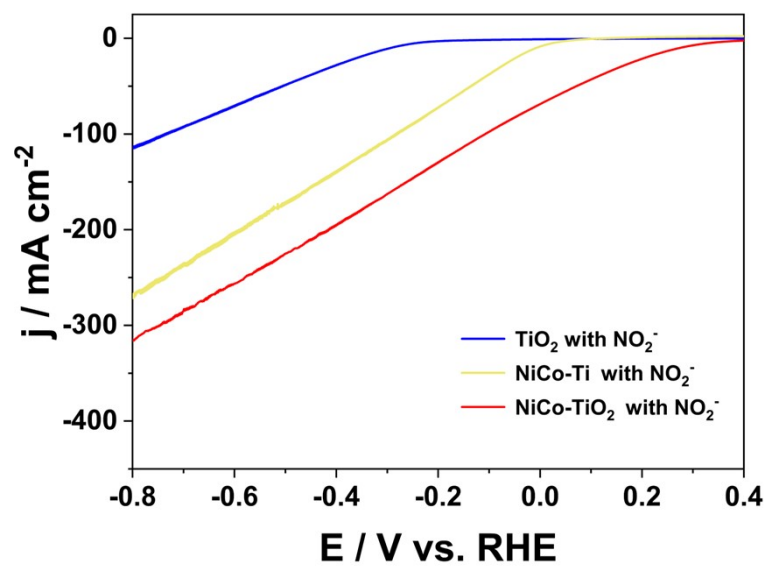
Fig. S4 XPS spectrum of Ni element in Ni-TiO$_2$.

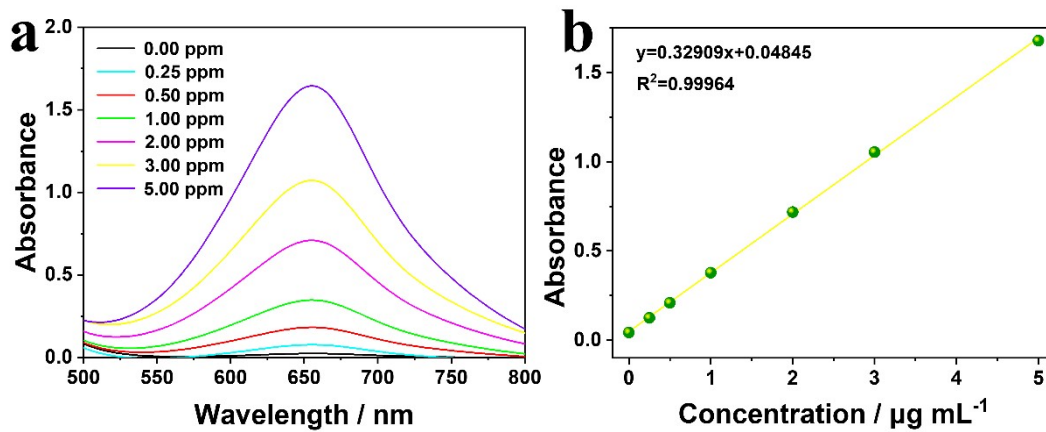Fig. S5 LSV curves of NiCo-TiO$_2$, NiCo-Ti, and TiO$_2$.

Fig. S6 (a) UV-vis absorption spectra and corresponding (b) calibration curve used for calculation of NH$_3$ concentration.
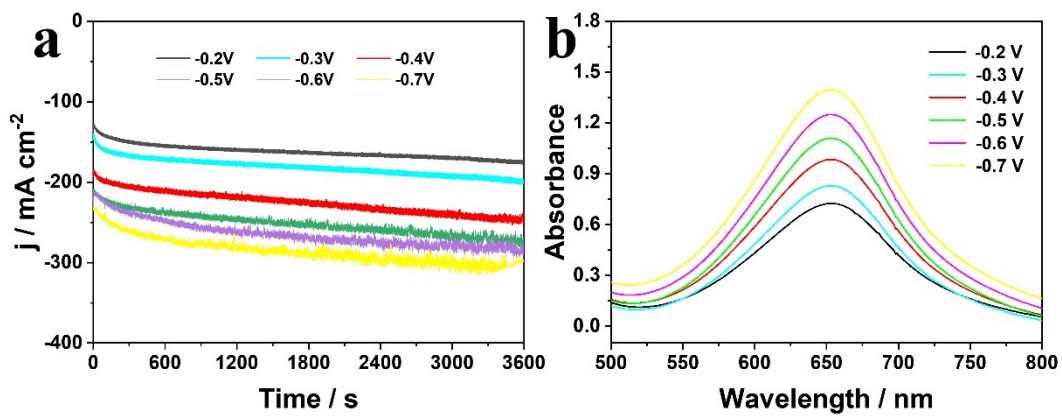
Fig. S7 (a) Chronoamperometry curves (from −0.2 V to −0.7 V) and (b) corresponding UV-vis absorption spectra of NiCo-TiO$_2$ for electrogenerated NH$_3$ at various potentials.
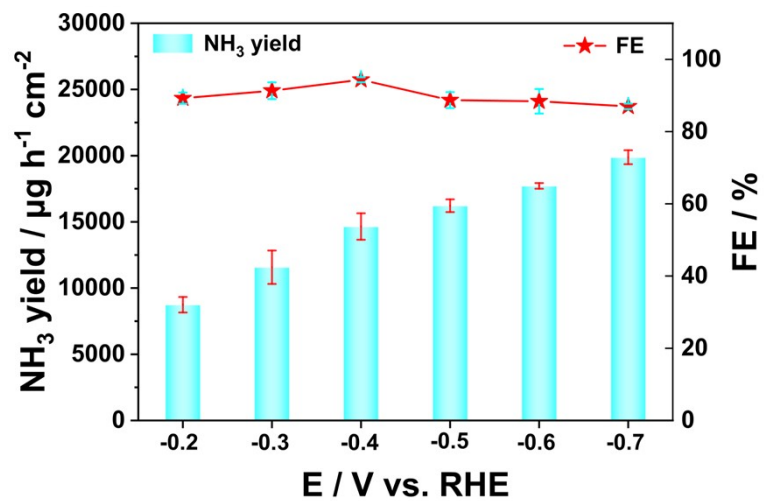
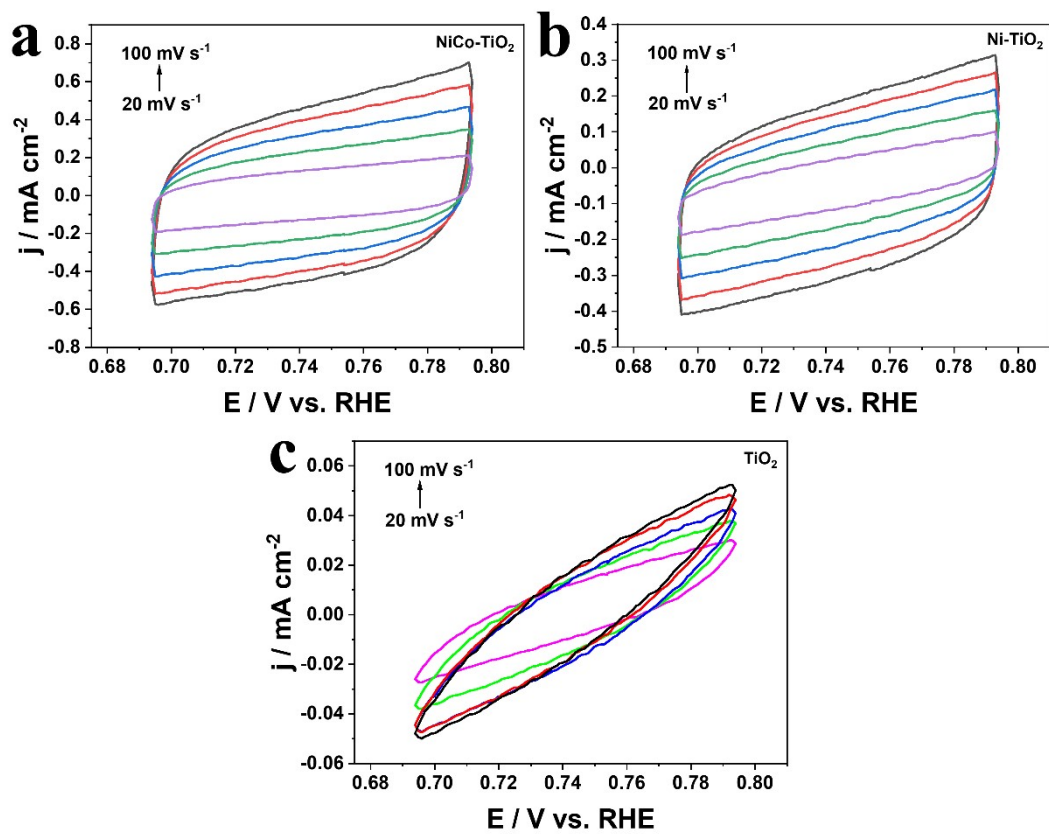Fig. S8 NH$_3$ yields and FEs of Ni-TiO$_2$ at different potentials.

Fig. S9 Cyclic voltammetry curves of NiCo-TiO$_2$, Ni-TiO$_2$ and TiO$_2$ at different scan rates (20, 40, 60, 80, and 100 mV s^{-1}).
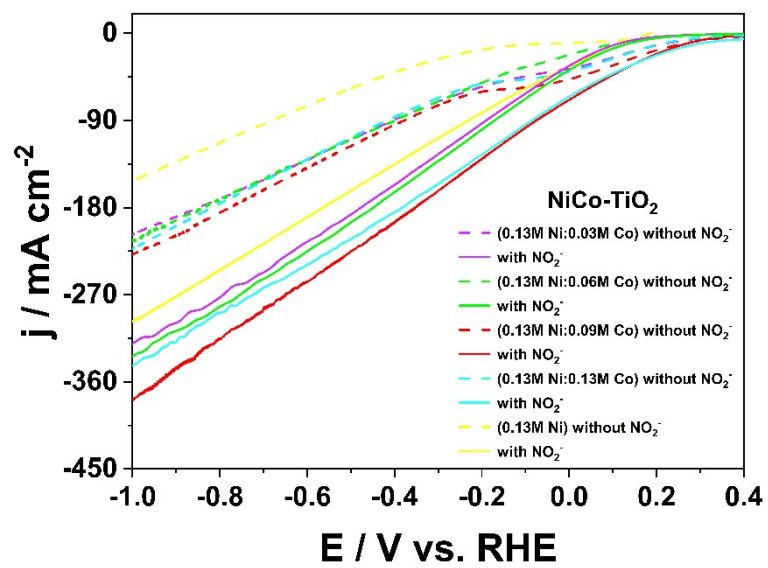
Fig. S10 LSV curve of NiCo-TiO$_2$ with different Ni/Co ratios in 0.1 M NaOH with and without 0.1 M NaNO$_2$
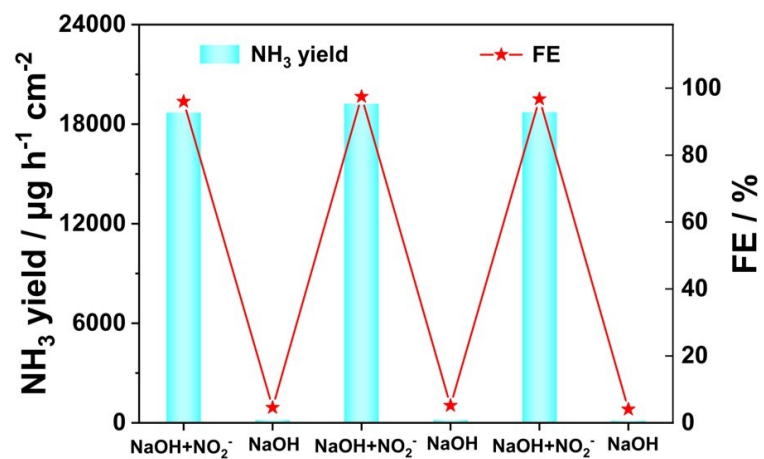
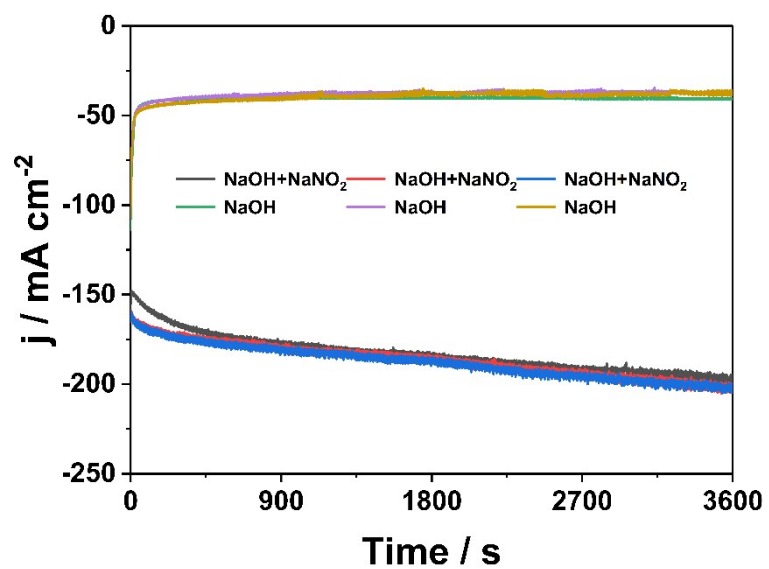Fig.S11 NH_3 yields and FEs of NiCo-TiO$_2$ during the alternating cycling tests.

Fig.S12 Chronoamperometry curves of NiCo-TiO$_2$ for NH$_3$ generation during the

alternating cycle experiments at –0.4 V.
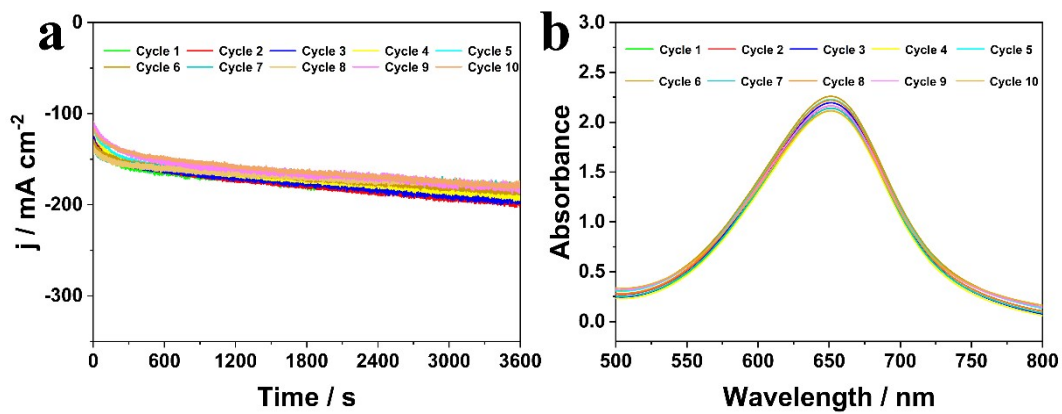
Fig. S13 (a) Chronoamperometry curves and (b) corresponding UV-vis absorption spectra of NiCo-TiO$_2$ for electrochemical catalytic production of NH$_3$ during recycling tests in 0.1 M NaOH with 0.1 M NO$_2^-$ at −0.4 V.
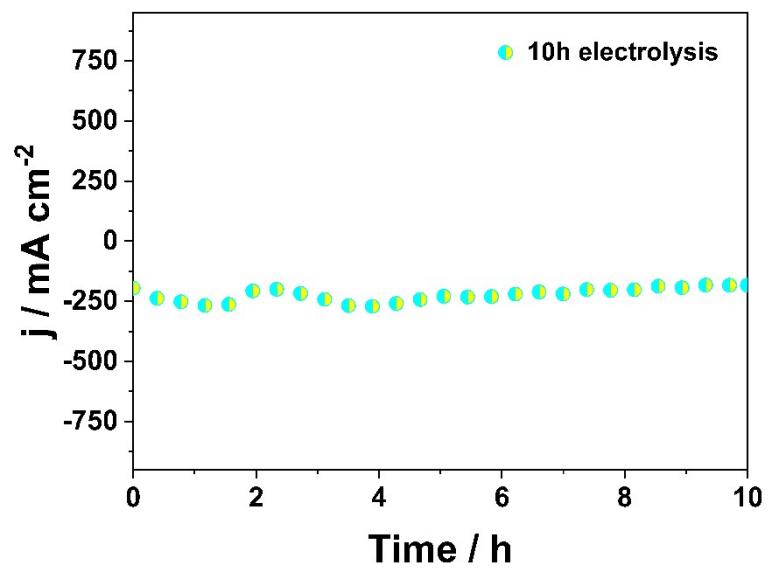
Fig. S14 Chronoamperometry curves of Ni-Mo-P/TiO$_2$ after 10 h electrolysis.

Fig. S15 LSV curves of NiCo-TiO$_2$ before and after 10 h electrolysis in 0.1 M NaOH with 0.1 M NO$_2^-$.

Fig. S16 XRD spectrum of NiCo-TiO$_2$ after continuous cycle tests.

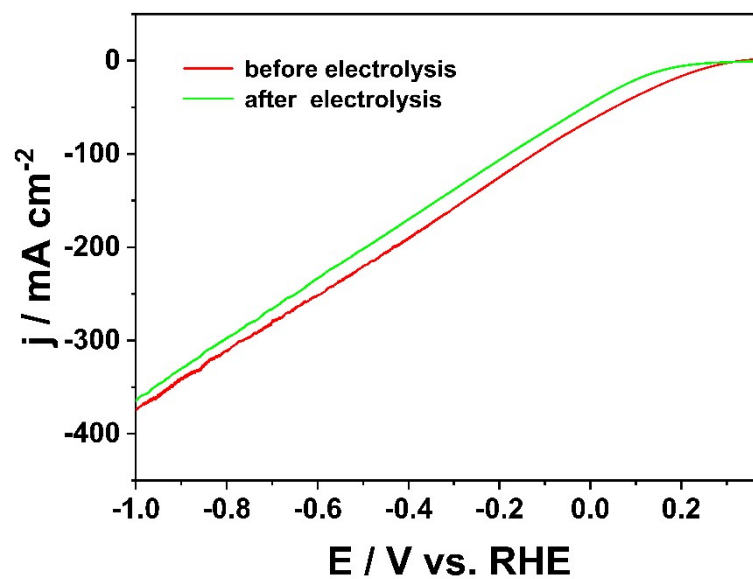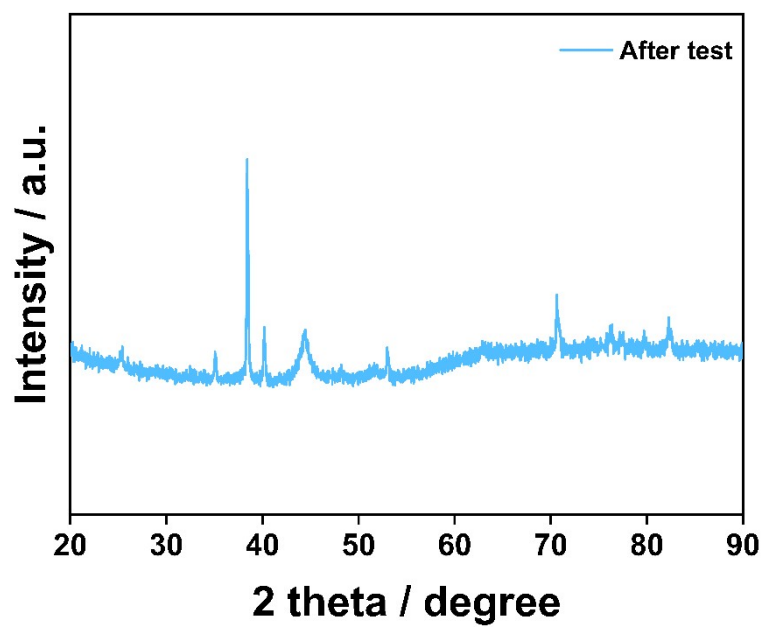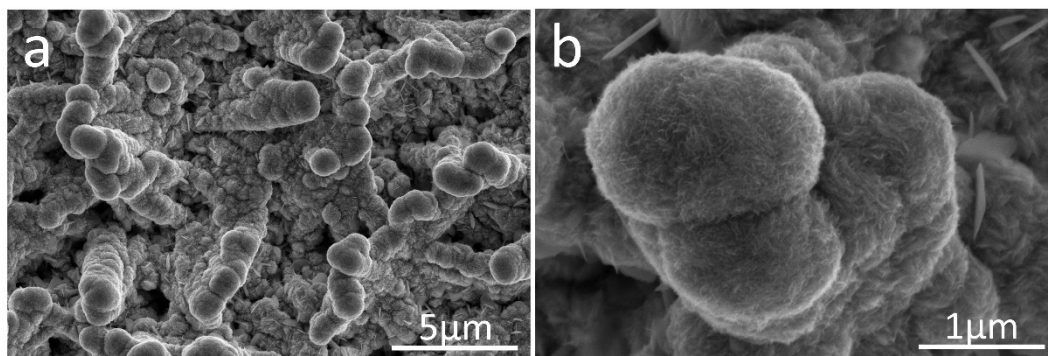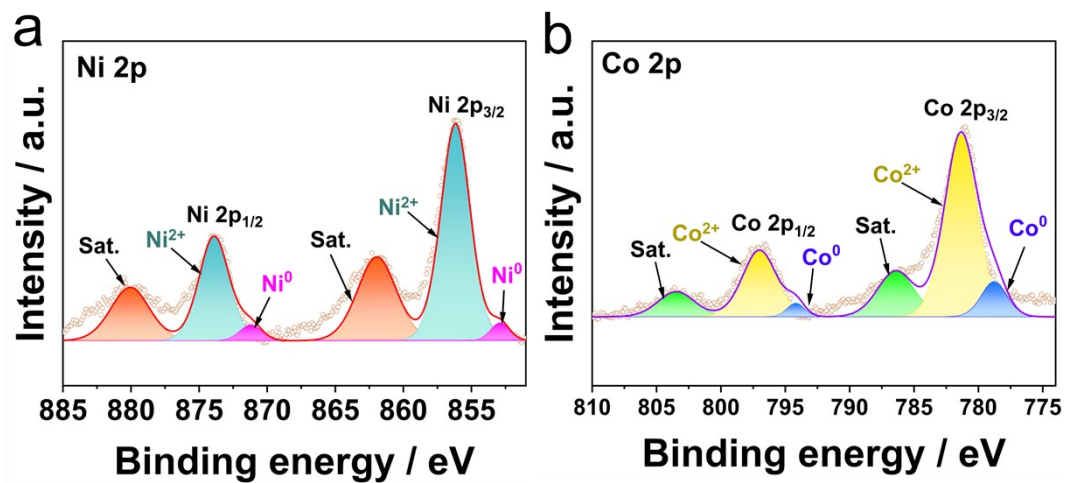Fig. S17 SEM images for NiCo-TiO$_2$ after NO$_2^-$RR electrolysis.

Fig. S18 The XPS spectra of (a) Ni 2p and (b) Co 2p regions of NiCo-TiO$_2$ after long-time electrolysis.

Table S1. Comparison of the catalytic performances of NiCo-TiO$_2$ with other reported

NO$_2^-$RR electrocatalysts under ambient conditions.

Catalyst	Electrolyte	Potential (V vs. RHE)	NH$_3$ yield (μg h^{-1}cm^{-2})	FE (%)	Ref.
NiCo-TiO$_2$	**0.1 M NaOH (0.1 M NO$_2^-$)**	**−0.4V**	**18736.2**	**97.5%**	**This work**
V-TiO$_2$/TP	0.1 M NaOH (0.1 M NO$_2^-$)	−0.6V	7083.9	93.2%	1
Ni@TiO$_2$/TP	0.1 M NaOH (0.1 M NO$_2^-$)	−0.5V	9667.8	98.5%	2
WO$_2$	0.1M NaOH (0.1 M NO$_2^-$)	−0.9V	14964.25	94.3%	3
Ni-Mo-P/TiO$_2$	0.1M NaOH (0.1 M NO$_2^-$)	−0.6V	16124.76	95.6%	4
MoO$_2$	0.5 M Na$_2$SO$_4$ (0.1 M NO$_2^-$)	−0.8V	8678.4	94.5%	5
NiWO$_4$	0.1M NaOH (0.1 M NO$_2^-$)	−0.4V	10 974.36	97.6%	6
NiS$_2$@TiO$_2$	0.1 M NaOH (0.1 M NO$_2^-$)	−0.5V	8251.8	92.1%	7
Ni$_2$P nanosheet	0.1 M PBS (200 ppm NO$_2^-$)	−0.3V	2692.2	90.2%	8
P-doped TiO$_2$	0.1 M Na$_2$SO$_4$ (0.1 M NO$_2^-$)	−0.6V	9533.6	90.6%	9
Cu$_3$P@TiO$_2$	0.1 M NaOH 0.1M NaNO$_2$	−0.7V	22212.2	97.1%	10
A-TiO$_{2-X}$	0.1 M NaOH (0.1 M NO$_2^-$)	−0.8V	12,230.1	91.1%	11

Ni-TiO$_2$/TP	0.1 M NaOH (0.1 M NO$_2^-$)	−0.5V	6464.56	94.89%	12
CF@Cu$_2$O	0.1 M PBS (0.1 M NO$_2^-$)	−0.6V	7510.73	94.21%	13
Ni@MDC	0.1 M NaOH (0.1 M NO$_2^-$)	−0.8V	5100	65.4%	14
Cu@TiO$_2$	0.1 M Na$_2$SO$_4$ (0.1 M NO$_2^-$)	−0.6V	8642.8	95.3%	15
TiO$_{2-x}$	0.1 M K$_2$SO$_4$ (0.1 M NO$_2^-$)	−0.7V	7898	92.7%	16
Ag@TiO$_2$/TP	0.1 M NaOH (0.1 M NO$_2^-$)	−0.5V	8743.1	96.4%	17
NiCu@TiO$_2$	0.1 M NaOH (0.1 M NO$_2^-$)	−0.5V	11712.49	96.25%	18

References

1. H. Wang, F. Zhang, M. Jin, D. Zhao, X. Fan, Z. Li, Y. Luo, D. Zheng, T. Li, Y. Wang, B. Ying, S. Sun, Q. Liu, X. Liu and X. Sun, *Mater. Today Phy.*, 2023, **30**, 100944.

2. X. Ji, C. Ma, F. Zhang, X. He, X. Fan, J. Li, Z. Li, L. Ouyang, L. Zhang, T. Li, D. Zhao, Y. Wang, J. Zhang, Z. Cai, S. Sun, A. A. Alshehri, Q. Lu and X. Sun, *ACS Sustainable Chem. Eng.*, 2023, **11**, 2686-2691.

3. H. Qiu, Q. Chen, X. An, Q. Liu, L. Xie, J. Zhang, W. Yao, Y. Luo, S. Sun, Q. Kong, J. Chen and X. Sun, *J. Mater. Chem. A*, 2022, **10**, 24969-24974.

4. Z. Ren, Q. Chen, J. Zhang, X. An, Q. Liu, L. Xie, W. Yao, X. Sun and Q. Kong, *Mater. Today Phy.*, 2023, **36**, 101162.

5. G. Wang, Q. Chen, X. An, Q. Liu, L. Xie, J. Zhang, W. Yao, X. Liu, S. Sun, X. Sun and Q. Kong, *Colloid. Surf. A*, 2023, **657**, 130549.

6. H. Qiu, Q. Chen and J. J. I. C. F. Zhang, *Inorg. Chem. Front.*, 2023, **10**, 3909-3915.

7. X. He, L. Hu, L. Xie, Z. Li, J. Chen, X. Li, J. Li, L. Zhang, X. Fang, D. Zheng, S. Sun, J. Zhang, A. Ali Alshehri, Y. Luo, Q. Liu, Y. Wang and X. Sun, *J. Colloid Interf. Sci.*, 2023, **634**, 86-92.

8. G. Wen, J. Liang, L. Zhang, T. Li, Q. Liu, X. An, X. Shi, Y. Liu, S. Gao, A. M. Asiri, Y. Luo, Q. Kong and X. Sun, *J. Colloid Interf. Sci.*, 2022, **606**, 1055-1063.

9. L. Ouyang, X. He, S. Sun, Y. Luo, D. Zheng, J. Chen, Y. Li, Y. Lin, Q. Liu, A. M. Asiri and X. Sun, *J. Mater. Chem. A*, 2022, **10**, 23494-23498.

10. Z. Cai, D. Zhao, X. Fan, L. Zhang, J. Liang, Z. Li, J. Li, Y. Luo, D. Zheng, Y. Wang, T. Li, H. Yan, B. Ying, S. Sun, A. A. Alshehri, H. Yan, J. Xu, Q. Kong and X. Sun, *Small*, 2023, **19**, 2300620.

11. Z. Ren, Q. Chen, X. An, Q. Liu, L. Xie, J. Zhang, W. Yao, M. S. Hamdy, Q. Kong and X. Sun, *Inorg. Chem.*, 2022, **61**, 12895-12902.

12. Z. Cai, C. Ma, D. Zhao, X. Fan, R. Li, L. Zhang, J. Li, X. He, Y. Luo, D. Zheng,

Y. Wang, B. Ying, S. Sun, J. Xu, Q. Lu and X. Sun, *Mater. Today Energy*, 2023, **31**, 101220.

13.   Q. Chen, X. An, Q. Liu, X. Wu, L. Xie, J. Zhang, W. Yao, M. S. Hamdy, Q. Kong and X. J. C. C. Sun, *Chem. Chem. Commun.*, 2022, **58**, 517-520.

14.   X. He, X. Li, X. Fan, J. Li, D. Zhao, L. Zhang, S. Sun, Y. Luo, D. Zheng, L. Xie, A. M. Asiri, Q. Liu and X. Sun, *ACS Appl. Nano Mater.*, 2022, **5**, 14246-14250.

15.   L. Ouyang, X. Fan, Z. Li, X. He, S. Sun, Z. Cai, Y. Luo, D. Zheng, B. Ying, J. Zhang, A. A. Alshehri, Y. Wang, K. Ma and X. Sun, *Chem. Commun.*, 2023, **59**, 1625-1628.

16.   D. Zhao, J. Liang, J. Li, L. Zhang, K. Dong, L. Yue, Y. Luo, Y. Ren, Q. Liu, M. S. Hamdy, Q. Li, Q. Kong and X. Sun, *Chem. Commun.*, 2022, **58**, 3669-3672.

17.   X. Fan, X. He, X. Ji, L. Zhang, J. Li, L. Hu, X. Li, S. Sun, D. Zheng, Y. Luo, Y. Wang, L. Xie, Q. Liu, B. Ying and X. Sun, *Inorg. Chem. Front.*, 2023, **10**, 1431-1435.

18.   L. Cai, A. Zhang, Y. Liang, X. Fan, X. He, C. Yang, L. Ouyang, D. Zheng, S. Sun, Y. Luo, Q. Liu, S. Alfaifi, A. Farouk, M. S. Hamdy, W. Zheng, Q. Kong and X. Sun, *Mater. Today Energy*, 2023, **38**, 101428.